Quantum Dynamical Simulations as a Tool for Predicting Photoinjection Mechanisms in Dye-Sensitized TiO2 Solar Cells

ARTICLE *in* JOURNAL OF PHYSICAL CHEMISTRY LETTERS · AUGUST 2012

Impact Factor: 7.46 · DOI: 10.1021/jz300880d

7 AUTHORS, INCLUDING:

Belen Oviedo
University of California, Riverside
17 PUBLICATIONS **95** CITATIONS
SEE PROFILE

Ximena Zarate
Universidad Autónoma De Chile
32 PUBLICATIONS **89** CITATIONS
SEE PROFILE

Ramiro Arratia-Perez
Universidad Andrés Bello
149 PUBLICATIONS **1,200** CITATIONS
SEE PROFILE

Cristián Gabriel Sánchez
National University of Cordoba, Argentina
60 PUBLICATIONS **890** CITATIONS
SEE PROFILE

THE JOURNAL OF PHYSICAL CHEMISTRY Letters

Letter

pubs.acs.org/JPCL

Quantum Dynamical Simulations as a Tool for Predicting Photoinjection Mechanisms in Dye-Sensitized TiO_2 Solar Cells

M. Belén Oviedo,[†] Ximena Zarate,[‡] Christian F. A. Negre,[†] Eduardo Schott,[‡] Ramiro Arratia-Pérez,[‡] and Cristián G. Sánchez*,[†]

[†]Departamento de Matemática y Física, Facultad de Ciencias Químicas, INFIQC, Universidad Nacional de Córdoba, Ciudad Universitaria, X5000HUA Córdoba, Argentina

[‡]Departamento de Ciencias Químicas, Facultad de Ciencias Exactas, Universidad Andres Bello, República 275, Santiago, Chile

ABSTRACT: On the basis of a time-dependent self-consistent density functional tight-binding (TD-DFTB) approach, we present a novel method able to capture the differences between direct and indirect photoinjection mechanisms in a fully atomistic picture. A model anatase TiO_2 nanoparticle (NP) functionalized with different dyes has been chosen as the object of study. We show that a linear dependence of the rate of electron injection with respect to the square of the applied field intensity can be viewed as a signature of a direct electron injection mechanism. In addition, we show that the nature of the photoabsorption process can be understood in terms of orbital population dynamics occurring during photoabsorption. Dyes involved in both direct (type-I) and indirect (type-II) mechanisms were studied to test the predictive power of this method.

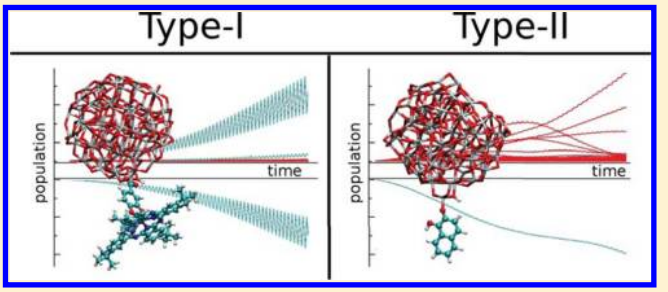

SECTION: Physical Processes in Nanomaterials and Nanostructures

Harvesting solar energy and photoconversion to electrical current with dye-sensitized solar cells (DSCs) was first proposed by O'Regan and Grätzel in 1991.[1] Since then, DSCs have become one of the most important topics of research in the field of clean and renewable energy.[1−5] DSCs can be viewed as a low-cost alternative energy source, where the challenge remains in building them from highly available and environmentally benign materials. These cells mainly constitute a sensitizer (organic or metal complex dye) that is attached to a nanocrystalline semiconductor film like TiO_2, ZnO, or SnO_2.[6−8] Sunlight is used as an energy source for photoexciting the dye, from which electrons are injected into the conduction band of the semiconductor. The dye is regenerated from its oxidized state by a redox couple such as I^-/I_3^- (other possible mediators are cobalt(II/III) complexes).[9,10] The electrolyte is infiltrated into a porous films, and it is regenerated by the reduction of the triiodide ions at the counter electrode, where electrons coming from the load of the circuit are supplied to complete the cycle. In this way, DSCs generate electricity from sunlight without chemical transformation of their components. Grätzel developed DSCs using ruthenium(II) bipyridyl (e.g., $[Ru(dcbpy)_2(NCS)_2]$ (N3)) and ruthenium(II) terpyridine (e.g., trithiocyanato(4,4′,4″-tricarboxy-2,2′,6′,2′-terpyridine)-ruthenium(II) ($Ru(tcterpy)(NCS)_3$ (black dye))[1−5,11] as the sensitizer dye, but it is relevant to mention that ruthenium is a very expensive metal and its sources are limited therefore, novel organic, inorganic, and/or organometallic dyes are desirable for highly efficient DSCs.

In the DSC photoinjection (PI) process, the main step is electron transfer from the dye molecule to the conduction band of the semiconductor. This process occurs following either one of two different mechanisms (type-I or indirect and type-II or direct injection mechanism) (Figure 1). The type-I process involves two steps that can be described as follows: an excitation from the ground state to the excited state of the dye, which is produced by the absorption of a photon, followed by an electron transfer to the conduction band of the semiconductor nanoparticle (NP). The type-II process is referred to the one-step electron injection from the ground state of the dye to the conduction band of the semiconductor upon photoabsorption.[12−18] In the type-II mechanism, a new charge-transfer band characterizes the direct electron excitation into the conduction band, and this can be observed by means of UV−vis spectra techniques. On the other hand, in type-I, (indirect injection mechanism), no new bands are observed in the UV−vis absorption spectrum. The most important parameter to be considered when studying the photoinjection process is the injection rate. Modern experimental techniques such as time-resolved laser spectroscopies, transient absorption spectroscopy, electron paramagnetic resonance, and terahertz spectroscopy have been useful to gain some insight into the mechanism and velocity of the injection step, but specific details of the whole process are still lacking.[8,19−24]

Received: July 4, 2012
Accepted: August 28, 2012

   dx.doi.org/10.1021/jz300880d | J. Phys. Chem. Lett. 2012, 3, 2548−2555

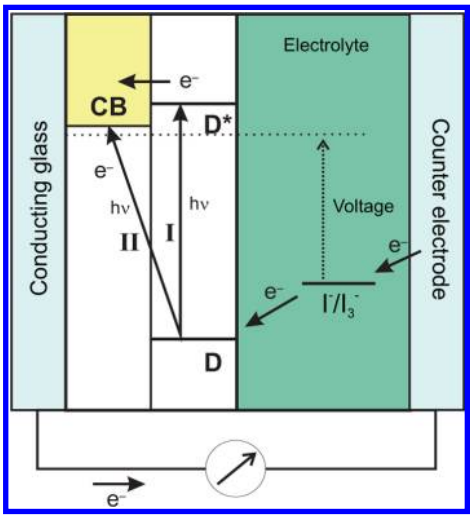

Figure 1. Electron injection mechanisms type-I and type-II in a DSC. CB: conduction band of the semiconductor. D: dye.

Nowadays, there is considerable interest in developing sensitizers that could show effective harnessing of the red and the near-IR portion of the sunlight spectra, to produce DSCs with the capability of covering a larger spectral region, mainly centered at the maximum of the solar emission spectrum.[25−29] Large sensitizers such as porphyrins and phenolphthalein have shown very promising properties for the design of solar cells due to their high extinction coefficients in the visible region of the UV−vis spectra. This kind of dye usually exhibits an indirect injection mechanism.[30,31]

Several theoretical studies of dyes anchored on different semiconductors employing a range of computer simulation techniques have been reported since the pioneering work of Rego et al. in 2003.[32−36] In recent work, Sánchez-de-Armas and co-workers studied the structural and electronic properties of different dyes on a $(TiO_2)_9$ cluster using TD-DFT. They described the main differences between the two mechanisms of electron injection, they showed the qualitative characteristics of the optical spectra, and they concluded that the indirect mechanism of photoinjection occurs through an orbital mainly

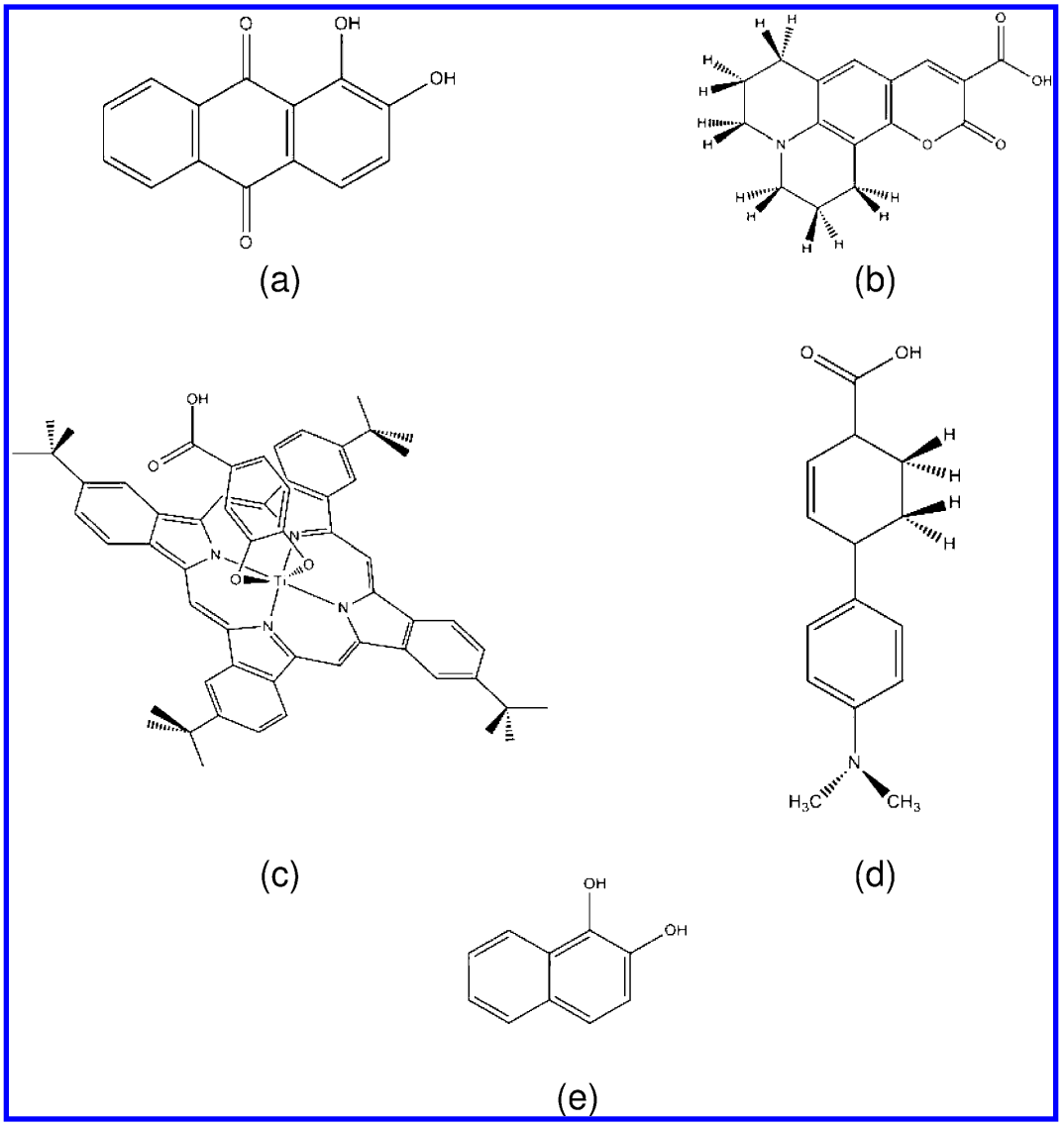

Figure 2. Studied compounds: alizarin (a), coumarin C343 (C343) (b), [Ti(Ph-tetra-*t*Bu)(catechol-CO2H)] (Pht-Ti) (c), aniline derivative (d), and naphthalenediol (Naph) (e).

dx.doi.org/10.1021/jz300880d | *J. Phys. Chem. Lett.* 2012, 3, 2548−2555

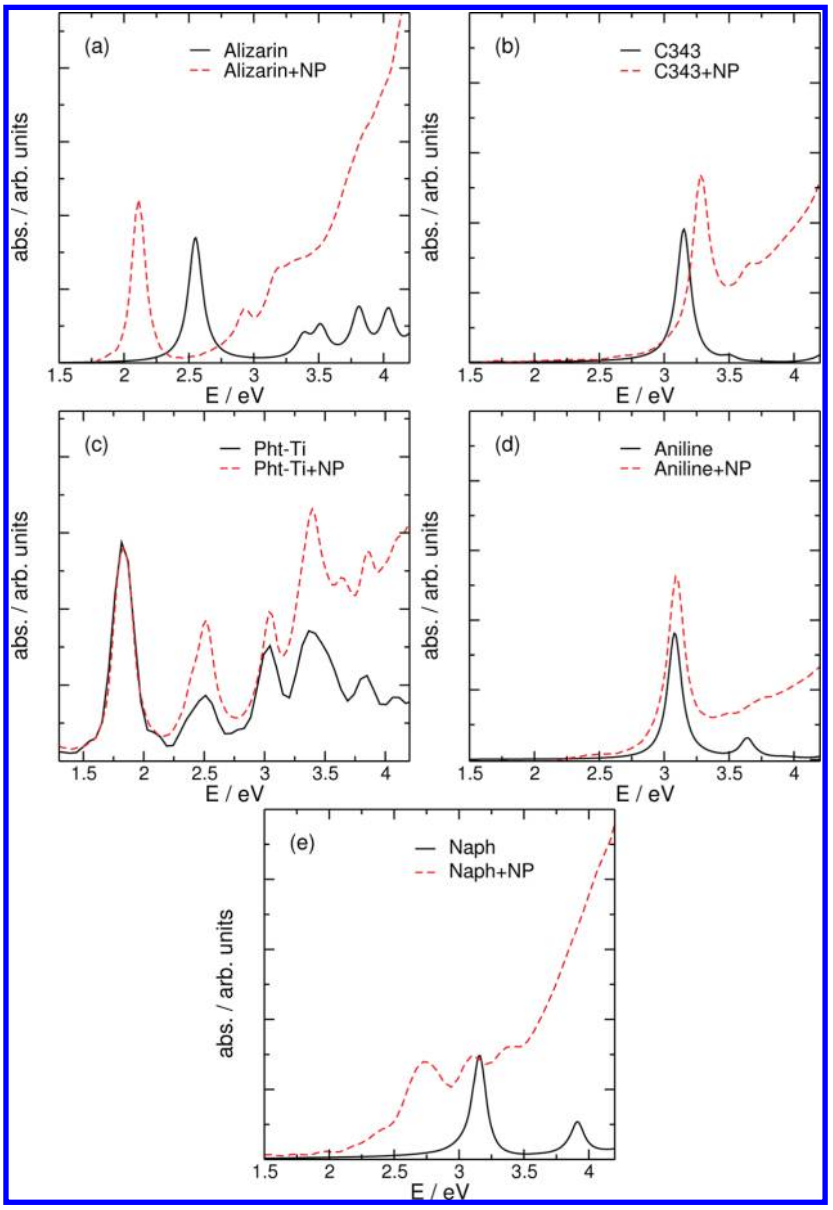

Figure 3. Superposition of the optical spectra of the free dyes (black lines) and dyes anchored to the TiO_2 NP (red lines). Alizarin (a), coumarin C343 (C343) (b), Pht-Ti (c), aniline derivative (d), and Naph (e).

localized in the molecule, very similar to the lowest unoccupied molecular orbital (LUMO) in the free dye. In contrast, the direct mechanism of electron injection requires strong electronic coupling between the conduction band of the semiconductor and the molecule because the excitation involves two orbitals that are localized in the dye and the semiconductor.[37]

Although the transfer across molecular−semiconductor interfaces has shown to be the research area of major interest in the DSC field, the whole time-dependent process is not fully understood. In this work, we pretend to shed light on the differences between the two photoinjection processes mentioned before by using a fully quantum theoretical treatment. To accomplish this task, we employ a family of sensitizers (Figure 2) that are anchored to the surface of a benchmark model anatase TiO_2 NP. This theoretical tool allows one to obtain a complete time-dependent picture of the photoelectron injection phenomenon from the electromagnetic wave striking the system to the further electron injection. A precise distinction between photoabsorption mechanisms was obtained from these time-dependent quantum dynamics simulations.

The methodology applied in this work has been widely described in refs 15, 38, and 39 and is based on the time propagation of the one electron density matrix under the influence of external time-varying electric fields in order to obtain optical information from the system. Essentially, it is a real time-dependent simulation, where the electronic structure is obtained from a density functional theory based tight-binding (DFTB) Hamiltonian. The DFTB+ code[40], which implements self-consistent DFTB, was used to model the electronic structure of the cluster−molecule system in its ground state, using *tiorg* - 0 - 1 and *mio*- 0 - 1 DFTB parameter sets.[41,42] Optical absorption spectra are obtained by introducing an initial perturbation in the shape of a Dirac delta pulse to the initial ground-state density matrix.[43] After pulse application, the evolution of the density matrix can be calculated by time integration of its equation of motion as described in refs 15, 38, and 39. In the linear response regime, when the applied electric

dx.doi.org/10.1021/jz300880d | J. Phys. Chem. Lett. 2012, 3, 2548−2555

field pulse is small, the complex polarizability can be obtained from deconvolution of the dipole moment signal from the excitation waveform after a Fourier transformation. The absorption spectrum is proportional to the imaginary part of the frequency-dependent polarizability. Calculation of the full average polarizability over the three Cartesian axes requires three independent determinations of the complex polarizability along these axes, which correspond to the direction of initial polarization. An exponential damping with a time constant of 10 fs is applied to the dipole moment signal, uniformly broadening all spectral lines. A deeper understanding of the nature of the excitation can be obtained from the time-dependent molecular orbital populations following a laser excitation in tune with the excitation energy.[39] This population can be obtained by rotation of the one-electron time-dependent density matrix to the molecular orbital basis. The diagonal elements of this rotated density matrix represent instantaneous molecular orbital populations, its off-diagonal elements representing coherences between different excitations.

The cluster structure used for all calculations is the same as that previously employed in ref 15 for the description of the photoinjection from catechol and cresol. This cluster consists of a 270 atom (90 TiO_2 units) anatase nanocluster, and this structure was taken from an equilibrated molecular dynamics simulation at 300 K. as described in ref 15.

We first proceeded by calculating the absorption spectra of the isolated dyes (Figure 2) and the dyes adsorbed onto the TiO_2 NP. Where all geometries were fully optimized employing DFTB for the isolated molecules, in the case of the adsorbed species, geometry optimization was restricted to the molecule and the nearest TiO_2 surrounding units. It is well-known that the difference between the two mechanisms of the electron injection in the DSCs can be appreciated from the absorption spectrum.[18,37] In the direct injection mechanism (type-II) a new band that corresponds to the charge-transfer excitation from the dye into the NP conduction band appears in the absorption spectrum of the dye adsorbed on the NP, whereas no new bands are observed in the case of the indirect mechanism (type-I).

Absorption spectra for the free dyes and dye−TiO_2 NP complexes are shown in Figure 3. From Table 1, it can be observed that the absorption energies are in good agreement with experimental data in the literature.[37,44−48] It is worth noting that the spectrum of the Pht-Ti shows the characteristic bands of a porphyrinic molecule[38] with a near-UV band (the Soret band) and the visible bands (Q bands), suggesting a strong absorption in the visible region, in fair accordance with previous experimental results.[46]

Table 1. Comparison of the Absorption Energy Values (eV) for Different Dyes on an Anatase TiO_2 Nanoparticle in Vacuum Obtained by the Method Described in the Text and with Experimental Values Found in the Literature

	free dye		dye + NP	
dye	TD-DFTB	exp. value	TD-DFTB	exp. value
alizarin	2.5	2.9[44]	2.1	2.47[44]
coumarin C343	3.1	2.81[45]	3.3	2.71[37]
Pht-Ti	1.8	1.77[46]	1.8	1.77[46]
aniline derivative	3.1	3.17[47]	3.1	3.55[47]
Naph	3.2	3.7[48]	2.7	1.2−3.2[37]

Alizarin, coumarin C343, Pht-Ti, and the aniline derivative (Figure 3a−d) are molecules that exhibit an indirect (type-I) mechanism for electron injection. This can be observed in the spectra of the dye−NP system, where no new absorption band appears in the visible region upon adsorbing the dye onto the TiO^2 NP. The lowest-energy band suffers a red shift for the alizarin−NP, while coumarin C343 shows a slight shift to higher energies, and no significant shift is observed for the aniline derivative and the Pht-Ti−NP. The lack of energy shift in this case can be attributed to the weak coupling between the states of the dye and those from the NP upon adsorption. Unlike the others dyes, Naph shows the appearance of a new optically active transition band in the visible region when adsorbed onto the NP. The same behavior was observed for catechol and cresol molecules in a a previous study.[15] For all cases of Figure 3, the sharp rise in the absorption region at high energy is produced by the excitation of electron−hole pairs within the TiO_2 NP.

It is worth noting that Naph and alizarin are similar molecules and have identical anchoring groups. From Table 1, it can be noted that the red shift of the absorption band for the alizarin−TiO_2 complex is about 0.4 eV; furthermore, the shift of the absorption band for the Naph−TiO_2 complex is 0.5 eV with respect to free dye absorption band. We assign the absorption band of the alizarin−TiO_2 complex to be the same as the band for the free dye because no broadening of the band is observed when the dye is adsorbed to the NP. In contrast, for the case of Naph, adsorption clearly causes the appearance of a band that is broadened with respect to that of the free dye. The local field at the surface of the NP is the cause of the larger red shift of the absorption band of alizarin−TiO_2. The difference in shifts can be explained from the fact that Naph is a smaller molecule and therefore the influence of the local field is stronger. This effect is smaller or negligible for molecules with larger spatial extent due to the short range of the field generated by the NP.

As noted, Naph and alizarin have close chemical structures and the same anchoring group. Why is it then that these two dyes present different injection mechanisms? The chemistry behind the difference between the two dyes can be understood as follows: The highest occupied molecular orbital (HOMO) of the dye is pinned to the upper edge of the valence band, simply from a principle of electron electrochemical potential equalization;[49] these are the states that are available to form bonds to the anchoring group. Considering that the band gap of the NP is basically constant, extending π conjugation in the dye moves the LUMO to lower energies, decoupling it from the conduction band.

Alizarin and Naph are two extreme examples in which this effect is clearly seen because they share the anchoring group, and therefore, the chemistry of the coupling with the NP is similar. As can be seen from Figure 3, the excitation energy in the case of alizarin is smaller than that of Naph and below the absorption edge, whereas in the case of Naph, the excitation is within the absorption edge.

Figure 4 shows the complex dye−TiO_2 for Naph (a) and alizarin (b) dyes, where the HOMO and LUMO are plotted; this figure shows the differences in the electronic excitations. The excitation of the Naph−TiO_2 complex occurs from the occupied state of the molecule to the unoccupied states of the conduction band of the NP; this is an excitation with charge transfer, whereas the electronic excitation of the alizarin−TiO_2 complex occurs in the dye.

dx.doi.org/10.1021/jz300880d | J. Phys. Chem. Lett. 2012, 3, 2548−2555

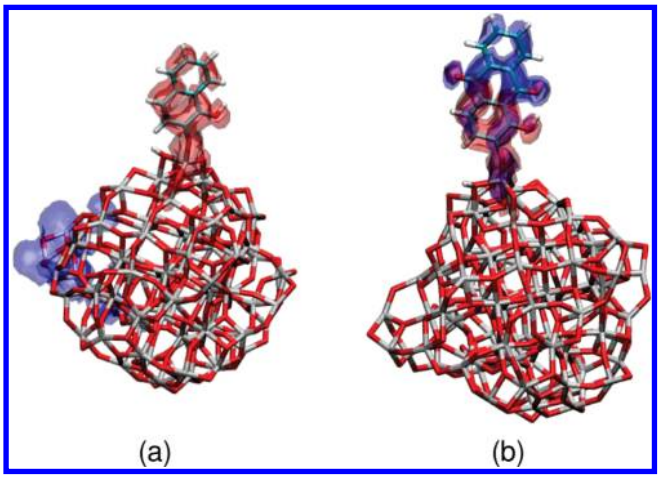

Figure 4. Plot of the HOMO (red) and the LUMO (blue) of (a) the Naph−TiO_2 complex and (b) the alizarin−TiO_2 complex superimposed on the respective atomic structures.

In previous work, we have shown that for a direct charge injection mechanism in a dye−NP complex, the variation of total Mulliken charges of the dye is proportional to the intensity of the applied field, that is, the current between the dye and the NP caused by illumination is a linear function of the square of the field strength.[15]

Here, we extend our previous results by comparing the variation of the current as a function of applied field for both direct and indirect injection mechanisms. Figure 5 shows the variation of the Mulliken charges for Naph (type-II) and Pht-Ti (type-I), adsorbed in the NP, when a laser-type electric field perturbation is applied. As observed from Figure 5a, Naph (type-II) has a linear dependence of the injection rate with the square of the applied field intensity. The latter behavior was seen for the case of catechol in our previous work.[15] On the other hand from Figure 5b, the Pht-Ti (type-I) dye shows a linear dependence with the cube of the intensity of the applied field for the variation of the cluster charge as a function of time. The magnitude of the slopes k_t in both processes are different, being larger for the type-II mechanism.

If we consider the dye−NP complex as a two-level system, of which the upper level is coupled to a manifold of states to which population can escape, the second-order behavior with respect to field intensity can be explained on the basis of quantum mechanical perturbation theory.[50,51] To first order in the field perturbation, when the exciting field is in tune with the electronic excitation of the two-level system, at short times, the population in the upper state grows with the square of time with a proportionality constant that depends on the square of the applied field.[52]

$$|P_{\text{upper}}|^2 = \frac{|\hat{\mu}E_0|^2}{4\hbar^2}t^2 \tag{1}$$

Incoherent escape from this level into the conduction band, up to first order in the coupling and at short times, can then be treated from simple first-order kinetics, in which the decay rate of the occupation in the upper level is proportional to its population.[50,51]

$$\frac{\mathrm{d}|P_{\text{upper}}|^2}{\mathrm{d}t} \propto |P_{\text{upper}}|^2 \tag{2}$$

This decay rate is the change in Mulliken populations plotted in Figure 5, which can now be seen to scale with the square of the applied field. We have verified this behavior from studying numerically the dynamics of a model two-level system coupled to a handfull of states. This represents the dynamics observed for type-II systems at short times.

On the other hand, for the case of Pht-Ti−TiO_2, a deeper analysis needs to be done in order to explain the third-order behavior. Third order is beyond perturbation theory, and a full explanation requires incorporating the change in electronic structure caused by the exciting field. In any case, the current as a function of applied field gives another way to distinguish between these two types of DSCs. A full explanation of the different dependencies on the applied field is very difficult in this fully atomistic picture that captures the photoinjection process in all of its time-dependent complexity. Further modeling is underway and will be the subject of a future publication.

In order to further investigate the injection mechanism, we studied the evolution of the density matrix in the molecular orbital basis set. (For a more detailed description on how to obtain the time dependent molecular orbital populations following a laser excitation in tune with the excitation energy please refer to Oviedo and Sánchez.[39]). This study provides a clear understanding of the nature of the excitation, which is crucial to characterize the type of injection mechanism in a DSC. Figure 6 shows the time-dependent molecular orbital

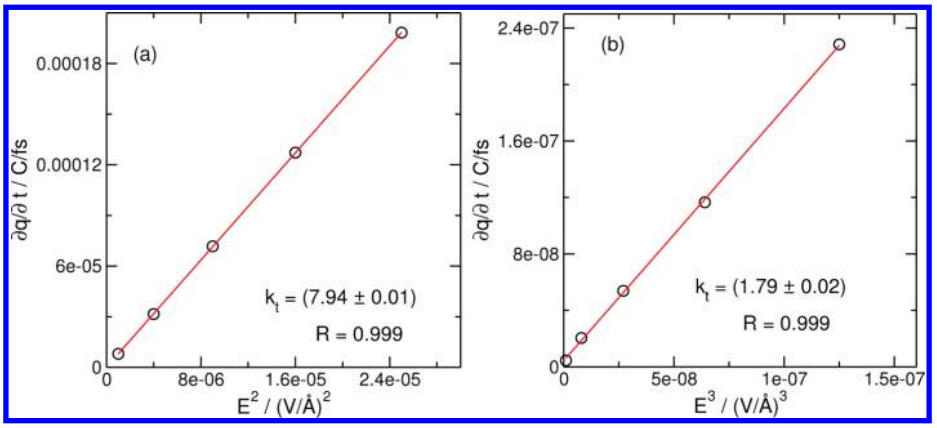

Figure 5. (a) Slope of the time-dependent averages of the Mulliken charges as a function of E^2 for Naph (type-II) and (b) E^3 for Pht-Ti (type-I). Straight lines are linear regressions to the data. Slopes (k_t) and correlation coefficients (R) are also shown in the figure.

dx.doi.org/10.1021/jz300880d | J. Phys. Chem. Lett. 2012, 3, 2548−2555

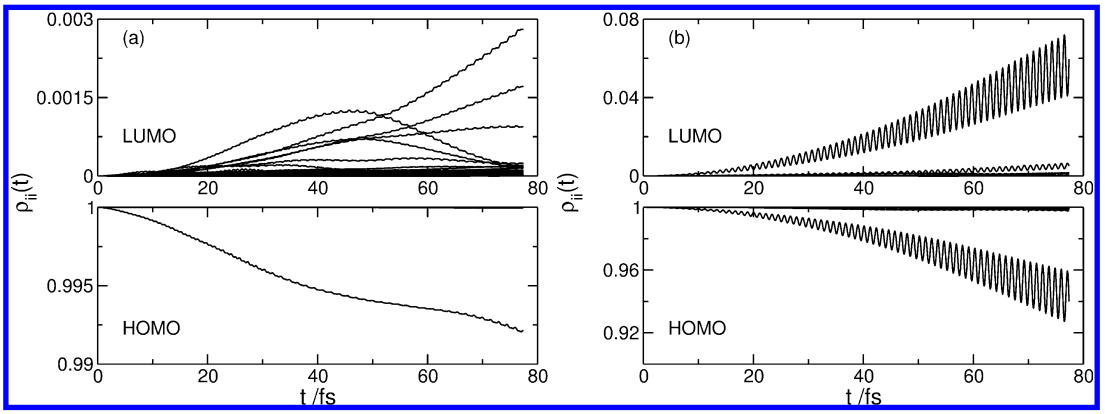

Figure 6. Population as a function of time for Naph−NP (a) and Pht-Ti−NP (b).

populations for Naph−NP (Figure 6a) and Pht-Ti−NP (Figure 6b) when a continuous laser-type perturbation in tune with the excitation energy is applied. The coherent and time-evolving superposition of states that results from continuous laser excitation is revealed by the oscillatory nature of the populations. From Figure 6, we can see that between both systems, the evolution of the population is remarkably different. When the system undergoes an indirect mechanism (Pht-Ti−NP) of electron injection, the largest changes of populations are in both the HOMO and LUMO. In contrast, for a direct injection mechanism (Naph−NP), there exist a population exchange between the HOMO and a broad manifold of high-energy states, where the excitation is delocalized.

As can be seen from Figure 6, the photoinjection times predicted by the calculation are slow compared with experimental results; this is within tens or hundreds of femtoseconds.[10] This deviation can be attributed to an effect comming from the differences in intensities of the field used in the calculation and the experiment. Also, this method does not take into account the phonon-assisted electron-transfer mechanisms. The inclusion of phonons that may speed up the process by trapping electrons within the NP is perhaps another element that may influence injection times and is now beyond the capabilities of the method. However, we believe that most of the quantum physics of the adiabatic step of electron injection is captured by the calculation.

In summary, in this work, we have proposed a new method for studying and predicting the photoinjection mechanisms in DSCs, based on time-dependent density functional tight-binding simulations. This method can reproduce the behavior of the absorption features when the dye is adsorbed onto a TiO_2 NP surface. The appearance of a new band is clearly observed for those dyes undergoing an indirect photoinjection mechanism (type-II). On the other hand, when the dye is of type-I, the absorption spectrum does not exhibit any new band upon adsorption. The latter is due to the weak coupling between the chromophore and the NP. By varying the field intensity when exciting the system with a laser-type perturbation, we showed that the photoinjection is no longer a second-order process when the system is classified as a type-I. Finally, we show that when the dye sensitizer is of type-II, the evolution of the molecular orbital population is of great complexity, showing an exchange from the HOMO to a manifold of high-energy orbitals from the conduction band of the NP. We believe that the detailed picture provided from the analysis of the molecular orbital population evolution can be of great value as this analysis can be extended to the description of different coupled dye−TiO_2 systems engineered for a DSC.

AUTHOR INFORMATION

Corresponding Author

*E-mail: cgsanchez@fcq.unc.edu.ar.

Notes

The authors declare no competing financial interest.

ACKNOWLEDGMENTS

We acknowledge support by Consejo Nacional de Investigaciones Científicas y Técnicas (CONICET) through Grant PIP 112-200801-000983. All calculations where performed with a generous time allocation on the *Cristina* supercomputer built with funding provided by ANPCYT through Grant PME-2006-01581. M.B.O. is grateful for a studentship from CONICET. X.Z., E.S., and R.A.-P. are grateful for the support by Proyecto P07-006-F de la Iniciativa Científica Milenio del Ministerio de Economía, Fomento y Turismo, CONICYT AT24100024 and for the Ph.D fellowships from CONICYT. X.Z. thanks Jorge Luis Zarate Bonilla.

REFERENCES

(1) O'Regan, B.; Grätzel, M. A Low-Cost, High-Efficiency Solar Cell Based on Dye-Sensitized Colloidal TiO_2 Films. *Nature* **1991**, *353*, 737−740.

(2) Bessho, T.; Yoneda, E.; Yum, J.-H.; Guglielmi, M.; Tavernelli, I.; Imai, H.; Rothlisberger, U.; Nazeeruddin, M. K.; Grätzel, M. New Paradigm in Molecular Engineering of Sensitizers for Solar Cell Applications. *J. Am. Chem. Soc.* **2009**, *131*, 5930−5934.

(3) Grätzel, M. Solar Energy Conversion by Dye-Sensitized Photovoltaic Cells. *Inorg. Chem.* **2005**, *44*, 6841−6851.

(4) Grätzel, M. Recent Advances in Sensitized Mesoscopic Solar Cells. *Acc. Chem. Res.* **2009**, *42*, 1788−1798.

(5) Grätzel, M. Photoelectrochemical Cells. *Nature* **2001**, *414*, 338−344.

(6) Beek, W.; Wienk, M.; Janssen, R. Hybrid Solar Cells from Regioregular Polythiophene and ZnO Nanoparticles. *Adv. Funct. Mater.* **2006**, *16*, 1112−1116.

(7) Kwong, C. Y.; Choy, W. C. H.; Djuri i, A. B.; Chui, P. C.; Cheng, K. W.; Chan, W. K. Poly(3-hexylthiophene):TiO2 Nanocomposites for Solar Cell Applications. *Nanotechnology* **2004**, *15*, 1156−1161.

(8) Yoshihara, T.; Katoh, R.; Furube, A.; Murai, M.; Tamaki, Y.; Hara, K.; Murata, S.; Arakawa, H.; Tachiya, M. Quantitative Estimation of the Efficiency of Electron Injection from Excited Sensitizer Dye into Nanocrystalline ZnO Film. *J. Phys. Chem. B* **2004**, *108*, 2643−2647.

(9) Privalov, T.; Boschloo, G.; Hagfeldt, A.; Svensson, P. H.; Kloo, L. A Study of the Interactions between I^-/I_3^- Redox Mediators and

Organometallic Sensitizing Dyes in Solar Cells. *J. Phys.Chem. C* **2009**, *113*, 783−790.
(10) Hagfeldt, A.; Boschloo, G.; Sun, L.; Kloo, L.; Pettersson, H. Dye-Sensitized Solar Cells. *Chem. Rev.* **2010**, *110*, 6595−6663.
(11) Ardo, S.; Meyer, G. J. Photodriven Heterogeneous Charge Transfer With Transition-Metal Compounds Anchored to TiO_2 Semiconductor Surfaces. *Chem. Soc. Rev.* **2009**, *38*, 115−164.
(12) De Angelis, F. Direct vs. Indirect Injection Mechanisms in Perylene Dye-Sensitized Solar Cells: A DFT/TDDFT Investigation. *Chem. Phys. Lett.* **2010**, *493*, 323−327.
(13) Tae, E. L.; Lee, S. H.; Lee, J. K.; Yoo, S. S.; Kang, E. J.; Yoon, K. B. A Strategy to Increase the Efficiency of the Dye-Sensitized TiO_2 Solar Cells Operated by Photoexcitation of Dye-to-TiO_2 Charge-Transfer Bands. *J. Phys. Chem. B* **2005**, *109*, 22513−22522.
(14) Koops, S. E.; Barnes, P. R. F.; O'Regan, B. C.; Durrant, J. R. Kinetic Competition in a Coumarin Dye-Sensitized Solar Cell: Injection and Recombination Limitations upon Device Performance. *J. Phys. Chem. C* **2010**, *114*, 8054−8061.
(15) Negre, C. F. A.; Fuertes, V. C.; Oviedo, M. B.; Oliva, F. Y.; Sánchez, C. G. Quantum Dynamics of Light-Induced Charge Injection in a Model Dye−Nanoparticle Complex. *J. Phys. Chem. C* **2012**, *116*, 14748−14753.
(16) De Angelis, F.; Fantacci, S.; Selloni, A. *Nanotechnology* **2008**, *19*, 424002.
(17) Duncan, W. R.; Stier, W. M.; Prezhdo, O. V. Ab Initio Nonadiabatic Molecular Dynamics of the Ultrafast Electron Injection across the Alizarin−TiO_2 Interface. *J. Am. Chem. Soc.* **2005**, *127*, 7941−7951.
(18) Duncan, W. R.; Prezhdo, O. V. Theoretical Studies of Photoinduced Electron Transfer in Dye-Sensitized TiO_2. *Annu. Rev. Phys. Chem.* **2007**, *58*, 143−184.
(19) Wang, Y.; Hang, K.; Anderson, N. A.; Lian, T. Comparison of Electron Transfer Dynamics in Molecule-to-Nanoparticle and Intramolecular Charge Transfer Complexes. *J. Phys. Chem. B* **2003**, *107*, 9434−9440.
(20) Anderson, N. A.; Lian, T. Ultrafast Electron Transfer at the Molecule−Semiconductor Nanoparticle Interface. *Annu. Rev. Phys. Chem.* **2005**, *56*, 491−519.
(21) Ramakrishna, G.; Ghosh, H. N.; Singh, A. K.; Palit, D. K.; Mittal, J. P. Dynamics of Back-Electron Transfer Processes of Strongly Coupled Triphenyl Methane Dyes Adsorbed on TiO_2 Nanoparticle Surface as Studied by Fast and Ultrafast Visible Spectroscopy. *J. Phys. Chem. B* **2001**, *105*, 12786−12796.
(22) Furube, A.; Katoh, R.; Hara, K.; Sato, T.; Murata, S.; Arakawa, H.; Tachiya, M. Lithium Ion Effect on Electron Injection from a Photoexcited Coumarin Derivative into a TiO_2 Nanocrystalline Film Investigated by Visible-to-IR Ultrafast Spectroscopy. *J. Phys. Chem. B* **2005**, *109*, 16406−16414.
(23) McNamara, W. R.; Snoeberger, R. C., III; Li, G.; Richter, C.; Allen, L. J.; Milot, R. L.; Schmuttenmaer, C. a.; Crabtree, R. H.; Brudvig, G. W.; Batista, V. S. Hydroxamate Anchors for Water-Stable Attachment to TiO_2 Nanoparticles. *Energy Environ. Sci.* **2009**, *2*, 1173.
(24) McNamara, W. R.; Snoeberger, R. C.; Li, G.; Schleicher, J. M.; Cady, C. W.; Poyatos, M.; Schmuttenmaer, C. a.; Crabtree, R. H.; Brudvig, G. W.; Batista, V. S. Acetylacetonate Anchors for Robust Functionalization of TiO_2 Nanoparticles with Mn(II)−Terpyridine Complexes. *J. Am. Chem. Soc.* **2008**, *130*, 14329−14338.
(25) Stockwell, D.; Yang, Y.; Huang, J.; Anfuso, C.; Huang, Z.; Lian, T. Comparison of Electron-Transfer Dynamics from Coumarin 343 to TiO_2, SnO_2, and ZnO Nanocrystalline Thin Films: Role of Interface-Bound Charge-Separated Pairs. *J. Phys. Chem. C* **2010**, *114*, 6560−6566.
(26) Nazeeruddin, M. K.; De Angelis, F.; Fantacci, S.; Selloni, A.; Viscardi, G.; Liska, P.; Ito, S.; Takeru, B.; Grätzel, M. Combined Experimental and DFT-TDDFT Computational Study of Photoelectrochemical Cell Ruthenium Sensitizers. *J. Am. Chem. Soc.* **2005**, *127*, 16835−16847.
(27) Lin, L.-Y.; Tsai, C.-H.; Wong, K.-T.; Huang, T.-W.; Hsieh, L.; Liu, S.-H.; Lin, H.-W.; Wu, C.-C.; Chou, S.-H.; Chen, S.-H.; et al. Organic Dyes Containing Coplanar Diphenyl-Substituted Dithienosilole Core for Efficient Dye-Sensitized Solar Cells. *J. Org. Chem.* **2010**, *75*, 4778−4785.
(28) Snaith, H. J.; Zakeeruddin, S. M.; Wang, Q.; Péchy, P.; Grätzel, M. Dye-Sensitized Solar Cells Incorporating a "Liquid" Hole-Transporting Material. *Nano Lett.* **2006**, *6*, 2000−2003.
(29) Pensack, R. D.; Asbury, J. B. Beyond the Adiabatic Limit: Charge Photogeneration in Organic Photovoltaic Materials. *J. Phys. Chem. Lett.* **2010**, *1*, 2255−2263.
(30) Imahori, H.; Umeyama, T.; Ito, S. Large π-Aromatic Molecules as Potential Sensitizers for Highly Efficient Dye-Sensitized Solar Cells. *Acc. Chem. Res.* **2009**, *42*, 1809−1818.
(31) Lin, C.-Y.; Wang, Y.-C.; Hsu, S.-J.; Lo, C.-F.; Diau, E. W.-G. Preparation and Spectral, Electrochemical, and Photovoltaic Properties of Acene-Modified Zinc Porphyrins. *J. Phys. Chem. C* **2010**, *114*, 687−693.
(32) Rego, L. G. C.; Batista, V. S. Quantum Dynamics Simulations of Interfacial Electron Transfer in Sensitized TiO_2 Semiconductors. *J. Am. Chem. Soc.* **2003**, *125*, 7989−7997.
(33) Duncan, W. R.; Prezhdo, O. V. Nonadiabatic Molecular Dynamics Study of Electron Transfer from Alizarin to the Hydrated Ti^{4+} Ion. *J. Phys. Chem. B* **2005**, *109*, 17998−18002.
(34) Duncan, W. R.; Prezhdo, O. V. Temperature Independence of the Photoinduced Electron Injection in Dye-Sensitized TiO_2 Rationalized by Ab Initio Time-Domain Density Functional Theory. *J. Am. Chem. Soc.* **2008**, *130*, 9756−9762.
(35) Rocca, D.; Gebauer, R.; De Angelis, F.; Nazeeruddin, M. K.; Baroni, S. Time-Dependent Density Functional Theory Study of Squaraine Dye-Sensitized Solar Cells. *Chem. Phys. Lett.* **2009**, *475*, 49−53.
(36) Jakubikova, E.; Snoeberger, R. C.; Batista, V. S.; Martin, R. L.; Batista, E. R. Interfacial Electron Transfer in TiO_2 Surfaces Sensitized with Ru(II)−Polypyridine Complexes. *J. Phys. Chem. A* **2009**, *113*, 12532−12540.
(37) Sánchez-de Armas, R.; Oviedo, J.; San Miguel, M. A.; Sanz, J. F. Direct vs Indirect Mechanisms for Electron Injection in Dye-Sensitized Solar Cells. *J. Phys. Chem. C* **2011**, *115*, 11293−11301.
(38) Oviedo, M. B.; Negre, C. F. A.; Sanchez, C. G. Dynamical Simulation of the Optical Response of Photosynthetic Pigments. *Phys. Chem. Chem. Phys.* **2010**, *12*, 6706−6711.
(39) Oviedo, M. B.; Sánchez, C. G. Transition Dipole Moments of the Qy Band in Photosynthetic Pigments. *J. Phys. Chem. A* **2011**, *115*, 12280−12285.
(40) Aradi, B.; Hourahine, B.; Frauenheim, T. DFTB+, A Sparse Matrix-Based Implementation of the DFTB Method. *J. Phys. Chem. A* **2007**, *111*, 5678−5684.
(41) Dolgonos, G.; Aradi, B.; Moreira, N. H.; Frauenheim, T. An Improved Self-Consistent-Charge Density-Functional Tight-Binding (SCC-DFTB) Set of Parameters for Simulation of Bulk and Molecular Systems Involving Titanium. *J. Chem. Theory Comput.* **2010**, *6*, 266−278.
(42) Elstner, M.; Porezag, D.; Jungnickel, G.; Elsner, J.; Haugk, M.; Frauenheim, T.; Suhai, S.; Seifert, G. Self-Consistent-Charge Density-Functional Tight-Binding Method for Simulations of Complex Materials Properties. *Phys. Rev. B: Condens. Matter Mater. Phys.* **1998**, *58*, 7260−7268.
(43) Yabana, K.; Bertsch, G. F. Time-Fependent Local-Density Approximation in Real Time. *Phys. Rev. B: Condens. Matter Mater. Phys.* **1996**, *54*, 4484−4487.
(44) Duncan, W. R.; Prezhdo, O. V. Electronic Structure and Spectra of Catechol and Alizarin in the Gas Phase and Attached to Titanium. *J. Phys. Chem. B* **2005**, *109*, 365−373.
(45) Hara, K.; Sato, T.; Katoh, R.; Furube, A.; Ohga, Y.; Shinpo, A.; Suga, S.; Sayama, K.; Sugihara, H.; Arakawa, H. Molecular Design of Coumarin Dyes for Efficient Dye-Sensitized Solar Cells. *J. Phys. Chem. B* **2003**, *107*, 597−606.
(46) Palomares, E.; Martinez-Diaz, M. V.; Haque, S. a.; Torres, T.; Durrant, J. R. State Selective Electron Injection in Non-Aggregated

Titanium Phthalocyanine Sensitised Nanocrystalline TiO_2 Films. *Chem. Commun.* **2004**, 2112−2113.
(47) Chen, K.-F.; Hsu, Y.-C.; Wu, Q.; Yeh, M.-C. P.; Sun, S.-S. Structurally Simple Dipolar Organic Dyes Featuring 1,3-Cyclohexadiene Conjugated Unit for Dye-Sensitized Solar Cells. *Org. Lett.* **2009**, *11*, 377−380.
(48) Daglish, C. The Ultraviolet Absorption Spectra of some Hydroxynaphthalenes. *J. Am. Chem. Soc.* **1950**, *72*, 4859−4864.
(49) Schmickler, W.; Santos, E. *Interfacial Electrochemistry*; Springer: New York, 2010; p 282.
(50) Mukamel, S. *Principles of Nonlinear Optical Spectroscopy*, new edition ed.; Oxford Series on Optical and Imaging Sciences; Oxford University Press: New York, 1999.
(51) Nitzan, A. *Chemical Dynamics in Condensed Phases: Relaxation, Transfer, and Reactions in Condensed Molecular Systems (Oxford Graduate Texts)*; Oxford University Press: New York, 2006; p 744.
(52) Gerry, C.; Knight, P. *Introductory Quantum Optics*; Cambridge University Press: New York, 2004; p 332.